

# Numerical Study of Different Models for Turbulent Flow in 90° Pipe Bend

Rilwan Kayode Apalowo<sup>1</sup>




<sup>1</sup>Mechanical Engineering Department, Federal University of Technology Akure, Nigeria  
([rkapalowo@futa.edu.ng](mailto:rkapalowo@futa.edu.ng)) ORCID [0000-0002-4816-4931](https://orcid.org/0000-0002-4816-4931)

## Abstract

The investigation of the turbulence statistics for single-phase turbulent flow around 90° pipe bends have mainly been experimental. Considering the cost-effectiveness of the numerical computational fluid dynamics (CFD) compared to experimental measurement, this work aims to study the accuracies of different CFD models, and establish their functionality and limitations. This paper investigates the capabilities of different numerical turbulence models and spatial discretization schemes for CFD analysis of a 90° pipe bend. The pipe has a curvature radius which is seven times the inside diameter and a Reynolds number of 34132. The numerical modelling was developed on the commercial CFD software, ANSYS Fluent, evaluating the following viscous models:  $k - \varepsilon$ ,  $k - \omega$ , Spalart-Allmaras and Reynolds Stress Models. The streamwise velocities of the flow at cross-stream planes along the bend at 45° and 75° were computed for each of the turbulence models under different discretization schemes. The numerical results were compared against the existing experimental data for streamwise velocity, in order to investigate the accuracies of the different models. The results showed that the realizable  $k - \varepsilon$  and Spalart-Allmaras models exhibited the best agreements with the experimental measurements, with respective average errors of 3.83% and 3.27% under the first-order spatial discretization scheme. It was also observed that the velocity profiles obtained through the  $k - \omega$  models (Standard and BSL), Transition SST and Reynolds Stress models exhibited better correlation with the experimental velocity profiles within the velocity transition region.

**Author Keywords.** Numerical Simulation, CFD, Turbulent Flow, Turbulence Models, Streamwise Velocity, Pipe Bend.

**Type:** Research Article

 Open Access  Peer Reviewed  CC BY

## 1. Introduction

Circular cross section pipes are the most prominent and widely used fluid networks in fluid engineering. The bends along the circular pipe profile promote flexibility in the flow network. These bends have a significant effect on the profile and behaviour of fluids as they travel through them. The change in fluid profile, around the bend, can cause pressure drop, heat and mass transfer, which are significant interest phenomena in thermofluid engineering. Understanding these changes help improve and optimize the design of pipe bends for different applications. There are different turbulence models that can describe the turbulence phenomena in the pipe bends. A deep understanding of the different turbulence models functionality and limitations will aid an appropriate selection of a model for a specific simulation (Dutta et al. 2016).

The investigation of turbulent flow in curved pipe channel has been performed using different techniques, such as experimental measurement, theoretical approach, numerical modelling and simulation. Experimental techniques mainly include the Laser-Doppler (LDV)

measurement (al-Rafai, Tridimas, and Woolley 1990; Enayet et al. 1982), hot-wire anemometry (Azzola et al. 1986; Lee, Choi, and Han 2007) and Pitot tube measurement (Rowe 1970). al-Rafai, Tridimas, and Woolley (1990) performed Laser-Doppler (LDV) measurement of turbulent flow in 90° pipe bends and determined the influence of the bend curvature on the flow statistics. It was established that secondary flows are stronger in pipes with smaller bend. Enayet et al. (1982) also conducted LDV measurement of turbulent flow in a 90° pipe bend. The mean streamwise velocity, turbulence intensity and static pressure of the turbulent flow were measured at different cross-stream angles. LDV measurements for turbulent flow in a U-bend pipe was performed by Azzola et al. (1986). The root mean square (r.m.s) and azimuthal velocity components of the turbulent flow were computed downstream the bend. The contribution of Azzola et al. (1986) was extended by Lee, Choi, and Han (2007) to perform flow statistic measurements at different cross-stream angles in a 180 bend using hot-wire anemometry. Similarly, Anwer, So, and Lai (1989) and Anwer and So (1990) performed hot-wire anemometry measurement for turbulent flow in a U-bend. Turbulence statistics were measured at different angles up and down-stream the bend. Investigation of turbulent flow in 90° and 180° pipe bends was performed by Sudo, Sumida, and Hibara (1998, 2000) using the rotating hot-wire anemometry measurements. The turbulent statistics of the flow, such as the r.m.s. and mean streamwise velocities, were computed.

Theoretical and numerical models have also been implemented to investigate turbulent flow in curved pipes. Boersma and Nieuwstadt (1996) developed a Large Eddy Simulation (LES) based model to compute the mean velocity of a fully-developed turbulent flow in a pipe bend, and established the effect of the bend curvature on the mean velocity profile of the flow. Spedding, Benard, and McNally (2004) proposed empirical methods for computing pressure drop of turbulent flow in elbow pipe bends. Schiestel (2010) developed a statistical model for turbulent flow at various degrees of turbulence complexity in a pipe bend. Various numerical models have been employed to predict the flow statistics of turbulent flow in curved pipes. These include the Reynolds-averaged Navier–Stokes (RANS) model (Wilcox 1994; Durbin and Pettersson-Reif 2011), Reynolds stress (RS) model (Noorani 2015; Röhrig, Jakirlić, and Tropea 2015), Eddy-viscosity (EV) model (Wallin and Johansson 2002) and renormalization group (RNG) model (Hilgenstock and Ernst 1996), k-epsilon ( $k - \varepsilon$ ) model (Rahimzadeh et al. 2012), RNG  $k - \varepsilon$  model (Hellstrom and Fuchs 2007) and k-omega ( $k - \omega$ ) model (Di Piazza and Ciofalo 2010).

Recently, with the advancement in numerical algorithm, Computational fluid dynamics (CFD) has been widely applied as numerical tool for investigating turbulent flow in curved pipes by many researchers. Röhrig, Jakirlić, and Tropea (2015) conducted a comparative assessment of the different computational approaches for turbulent flow through a 90° pipe bend using RANS and LES CFD models. Dutta et al. (2016) analysed the distribution of static pressure of single-phase turbulent flow at a symmetry plane of pipe bends using the  $k - \varepsilon$  turbulence model. The coefficient of turbulent viscosity for single phase flow in pipe bends using turbulence kinetic energy and dissipation ratio are studied in Homicz (2004), Rahimzadeh et al. (2012), and Kim, Yadav, and Kim (2014). Crawford, Cunningham, and Spence (2007) carried out CFD modelling on a series of pipe bends with different curvature ratios of 1.3, 5 and 20 employing the standard  $k - \varepsilon$  model, realizable  $k - \varepsilon$  model,  $k - \omega$  model and a Reynolds stress model (RSM). It was established that RSM yielded the most accurate pressure loss data, followed by the realizable  $k - \varepsilon$  model, then the standard  $k - \varepsilon$  model, and finally the  $k - \omega$  model.

Previous studies on the investigation of turbulence flow parameters, such as the mean streamwise and root mean square velocities at different cross-stream angles, around a 90° pipe bend have mostly been experimental. Considering the cost implication, among other factors, of a fluid dynamics experimental rig and with the recent computational fluid dynamics technology providing efficient and cost-effective numerical solutions, such as the ANSYS FLUENT, implementing a CFD numerical tool to investigate the turbulence flow would complement and extend the current literature.

In this work, the mean streamwise velocities, at different cross-stream angles around a 90° pipe bend, are computed employing different numerical turbulence models. The results obtained by these models are compared with the experimental measurements in order to analyse the accuracies of the different models and establish the functionality and limitations of the models.

## 2. Geometry and Numerical Methodology

### 2.1. Description of the study case

The dimensions and geometry of the pipe bend is presented in Figure 1. The pipe has a uniform diameter through its channel, with an inside diameter ( $D_1$ ) of 43mm. By taking the advantage of the symmetric geometry of the pipe, only a half round size of the pipe is modelled. From the inlet, a straight horizontal channel of length  $70D_1$  precedes the test bend to aid proper flow development before the fluid encounters the bend, which is of  $7D_1$  radius of curvature. The curvature ratio of the pipe bend is obtained through Equation (1)

$$C. R. = \frac{r_1}{r_c} \quad (1)$$

The curvature ratio is then computed as 1: 13.95. A similar straight vertical channel of length  $70D_1$  supersedes the bend. For the turbulent flow, air is introduced into the pipe at a bulk velocity of 11.595 m/s and Reynolds number of 34132.

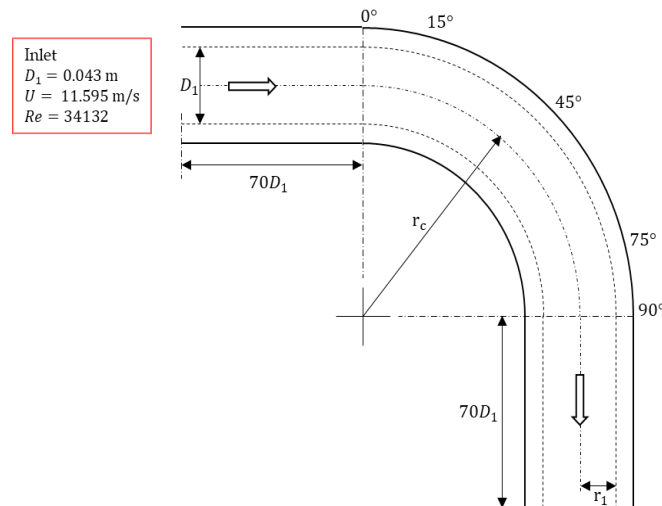


Figure 1: Schematic representation of the investigated 90° pipe bend

### 2.2. Mesh generation and grid independence analysis

The pipe geometry was created using the ANSYS Design-Modeler, and by taking the advantage of its symmetric geometry, only a half section of the pipe is modeled in order to reduce the computational cost. The mesh was created in ANSYS ICEM using 3D structured hexahedral elements. A very high resolution of mesh was adapted for the bend and regions near the wall, to ensure the accuracy of the flow parameters (such as velocity and pressure) which changes

rapidly around these regions. The wall  $y^+$  was plotted to verify the mesh spacing and it ranged from  $3 < y^+ < 9$ . Consequently, since the standard wall function is applicable for  $y^+ > 30$ , then the enhanced wall treatment was preferred.

The quality of the mesh greatly influences the accuracy of the numerical simulation. A very fine mesh is computationally more efficient but time consuming. On the other hand, there is a great need to eliminate the dependence of the calculation results on the grid size, in order to ensure the results accuracy. Therefore, a balance needs to be established for the results accuracy, the mesh grid size and the independence of the results on the grid size needs to be established. A convergence test was conducted for the mesh grid independence by using different mesh size schemes. The outcome of the convergence test is presented in the Results and Discussion section.

### **2.3. Materials and boundary conditions**

The materials for the fluid and the solid pipe in this study were air and aluminium respectively. Conducting CFD analysis on the test bend requires the description of boundary conditions for each of its boundary surfaces. There are four boundary surfaces on the modelled pipe, identified as the inlet, outlet, wall, and symmetry.

The inlet boundary condition is the velocity inlet, which was evaluated from the Reynolds number  $Re$  and other parameters of the pipe and fluid properties using Equation (2).

$$U = \frac{\mu Re}{\rho D} \quad (2)$$

In Equation (2),  $\mu$  and  $\rho$  are the fluid viscosity and density, and  $D$  is the pipe diameter. The inlet velocity was computed as 11.595 m/s. Turbulence specification method of intensity and hydraulic diameter was applied at the inlet. Turbulent intensity of 5% was used and the hydraulic diameter  $D_h$  was calculated as 10.75 m using Equation (3).

$$D_h = \frac{4A}{P_w} \quad (3)$$

In Equation (3),  $A$  and  $P_w$  are the cross-sectional area and wetted perimeter of the pipe.

The outlet boundary condition is the pressure outlet with turbulence specifications, intensity and hydraulic diameter, similar to those of the velocity inlet. The outlet boundary was set at a gauge pressure of 0 Pa, backflow intensity of 5% and backflow hydraulic diameter of 10.75 mm. At the wall boundary surface, a stationary boundary condition was applied, with a roughness of 0 m, roughness constant of 0.5 and a no slip shear condition for the velocity. Symmetry boundary condition was applied at the symmetry surface, since half of the pipe geometry was being modelled.

### **2.4. Solution scheme and convergence**

The numerical computations conducted in this study applied the SIMPLE algorithm, which is based on finite volume discretization. Different discretization schemes, such as the first-order upwind, second-order upwind and QUICK, were used to analyze all forms of flow situations. The different schemes were used to achieve a range of accuracy and provide a basis for comparisons.

### **2.5. Numerical calculations and experimental validation**

The pipe geometry illustrated in Figure 1 is similar to the one used in the experimental measurement of turbulent flow in pipe bend, using laser Doppler anemometry, in al-Rafai, Tridimas, and Woolley (1990). The experimental results are used to validate the numerical predictions obtained in this study.

All numerical modelling and CFD calculations in this study are conducted in ANSYS 19.2. Numerical measurements of flow at different cross-stream planes along the full length of the bend were considered, in order to study the behaviour of the flow within those regions of the bend. Normalised mean streamwise velocities are computed along the plane of symmetry at 45° and 75° for different turbulence models, in order to investigate the accuracy of each model. The results of the stream wise velocity were normalized ( $W^*$ ) by the fluid bulk velocity of 11.595 m/s. The accuracy of each model was evaluated using the standard percentage error, computed as using the relation in Equation (4).

$$\% Error = \frac{\sum_{k=1}^N |W_{N,k}^* - W_{E,k}^*|}{\sum_{k=1}^N W_{E,k}^*} \times 100 \quad (4)$$

In Equation (4),  $W_{N,k}^*$  and  $W_{E,k}^*$  are respectively the numerical and experimental normalized mean streamwise velocities along the nodal points of the symmetry plane.  $N$  is the number of nodal points. Measurements of streamwise and root mean square velocities are also measured at 0° (entry), 15°, 45° and 90° cross-stream planes of the bend, to study the turbulent flow behaviour around the bend.

### 3. Numerical Results and Discussion

#### 3.1. Convergence test and mesh independence

Upon setting the solution criteria, a convergence criterion of 0.0001 was applied to converge the residuals to zero. The convergence is being observed closely and iteration can be stopped when there is no further displacement in the velocity magnitude plot as shown in Figure 2.

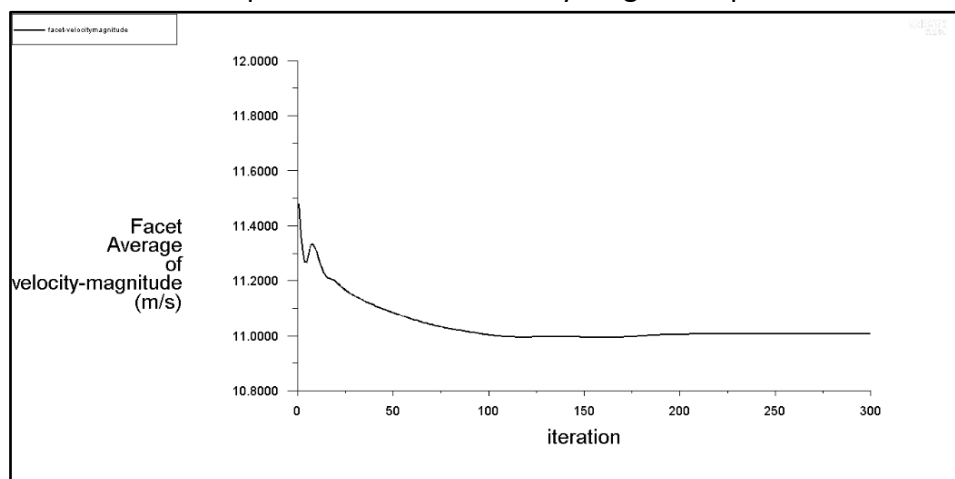


Figure 2: Convergence plot of velocity magnitude with respect to number of calculation iterations

The outcome of the convergence test conducted for the mesh grid independence by using different mesh size schemes is presented in Table 1. The normalised mean streamwise velocity calculated through each meshing scheme are compared against the experimental results obtained through Laser Doppler measurement in al-Rafai, Tridimas, and Woolley (1990).

Mesh Scheme	Number of Elements	Number of Nodes	% Deviation*
1	10,177	43,761	6.61
2	28,353	116,530	5.82
3	71,337	289,628	4.09
4	111,500	452,690	3.26
5	218,941	888,903	3.25
6	286,308	1,081,213	3.24

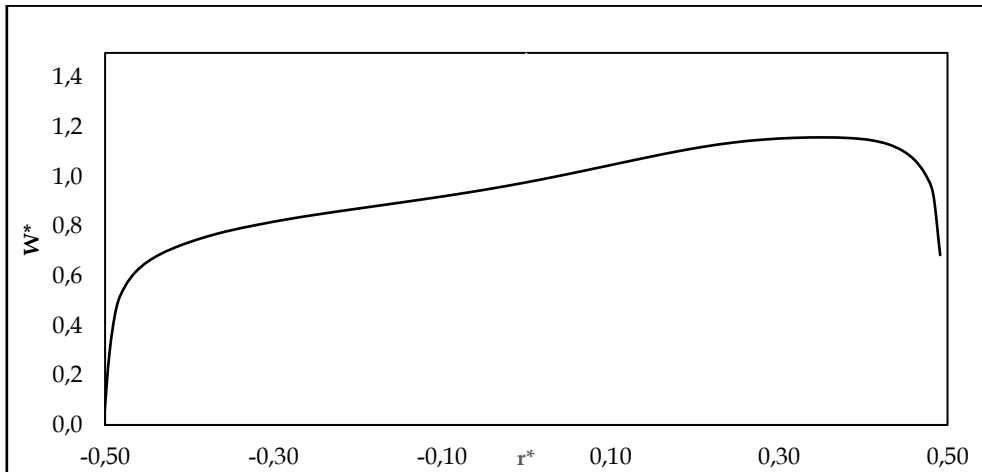
\*Experimental measurement as reference

Table 1: Mesh grid size convergence analysis based on streamwise velocity calculations

It was observed from [Table 1](#) that the result accuracy increases as the mesh element size reduces. Convergence was observed between the meshing schemes 4 and 6, in which their % deviations differ by just 0.02. Reducing the mesh size further would only increase the computational time without any significant improvement in the result accuracy. Therefore, the meshing scheme 4 was adopted for the calculations in this study.

### 3.2. Flow development

The air flow travels  $70D_1$  downstream through the pipe before entry the bend. The velocity profile of the flow development at the bend entry is presented in [Figure 3](#). The figure presents the normalised streamwise velocity ( $w^*$ ) profile against the normalised radial coordinate ( $r^*$ ). This profile shows that the flow has fully developed at the bend entry.



**Figure 3:** Flow development streamwise velocity profile at the bend entry

[Figure 4](#) presents the flow physics around the bend region, suggesting a secondary flow as a result of fluid acceleration and deceleration due to the pipe bend curvature. The outer wall region shows a high velocity and shear stress resulting from the impact of the fluid, as a result of higher turbulence of the fluid flow around the outer wall region. A velocity magnitude of 13.76 m/s was noticed at the outer wall region throughout the pipe bend.

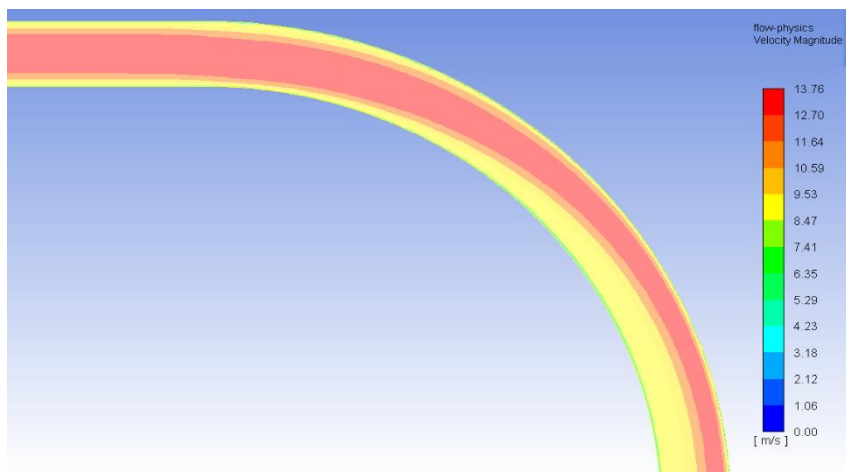


**Figure 4:** Flow physics velocity magnitude at the bend entry

### 3.3. Comparative analyses of different turbulence models

The mean streamwise velocity of the turbulent flow along the pipe bend under investigation was computed using different turbulence models. The numerical results of the streamwise velocities at different angles along the symmetry plane are compared with existing experimental results ([al-Rafai, Tridimas, and Woolley 1990](#)). Error analyses were conducted

for the comparisons. Turbulence models investigated include  $k - \varepsilon$ ,  $k - \omega$ , Spalart-Allmaras, Transition-SST and Reynold stress turbulence models. These models were investigated using different spatial discretization schemes. The results obtained by the different turbulent models and the discussions of the results are presented in the next sections.

### 3.3.1. $k - \varepsilon$ Model

The streamwise velocities at 45° and 75° around the bend, obtained through the standard, RNG and realizable  $k - \varepsilon$  turbulence models, using the second-order upwind discretization scheme are presented in Figure 5. Comparing the numerical results with the experimental measurements, an accuracy of 96.07% was obtained for the standard  $k - \varepsilon$  model, and 96.03% for the RNG and the realizable  $k - \varepsilon$  models at 45°. This indicates that the numerical predictions of the  $k - \varepsilon$  models are in good agreement with the experimental measurements. The accuracy levels of the different  $k - \varepsilon$  models are very close with a maximum difference of 0.04%.

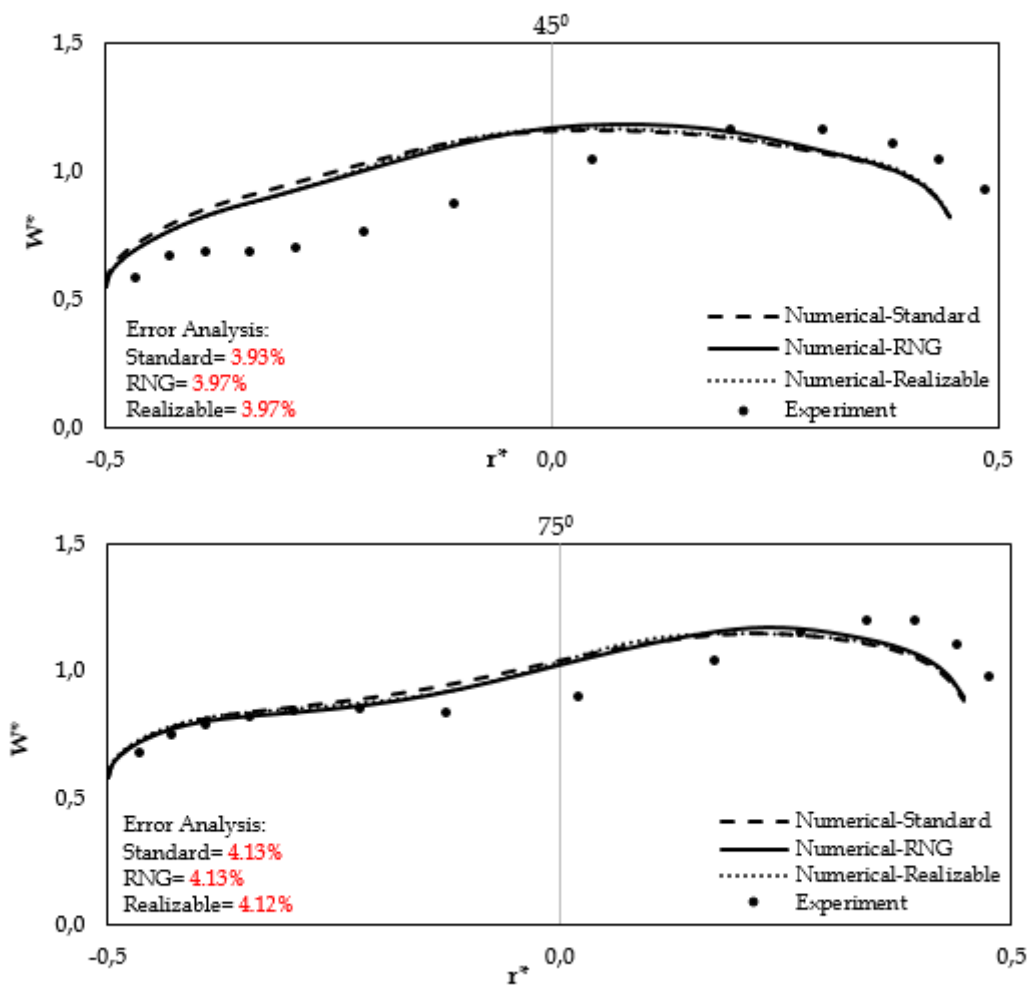


Figure 5: Normalized mean streamwise velocity plots obtained through the  $k - \varepsilon$  turbulence models

At 75°, the flow separation is much higher as it properly depicts the complex secondary flow features of the fluid, giving a more accurate information about the flow field, as presented in Figure 5. The accuracies of the different  $k - \varepsilon$  models are very close, with the realizable  $k - \varepsilon$  model having the highest accuracy of 95.88%.

However the average errors computed at 45° were observed to be lower compared to those obtained at 75° for the  $k - \varepsilon$  models, but the numerical velocity profiles represent the

experimental velocity profiles at 75° better than at 45°. In both cases, the velocity profiles by the RNG  $k - \varepsilon$  model were the closest to the experimental profiles.

### 3.3.2. $k - \omega$ Model

The streamwise velocities at 45° and 75° around the bend, obtained through the standard, BSL and SST  $k - \omega$  turbulence models, using the second-order upwind discretization scheme are presented in Figure 6. The results of the standard and the BSL models were similar and they showed more accuracy with % errors of 4.21 and 4.24 at 45° and 75° respectively. Although the two models showed a comparatively better accuracy compared to the SST  $k - \omega$  model, they however exhibit a lower accuracy of predicting the flow physics compared to the  $k - \varepsilon$  model at 75°, as validated with the experiment measurement.

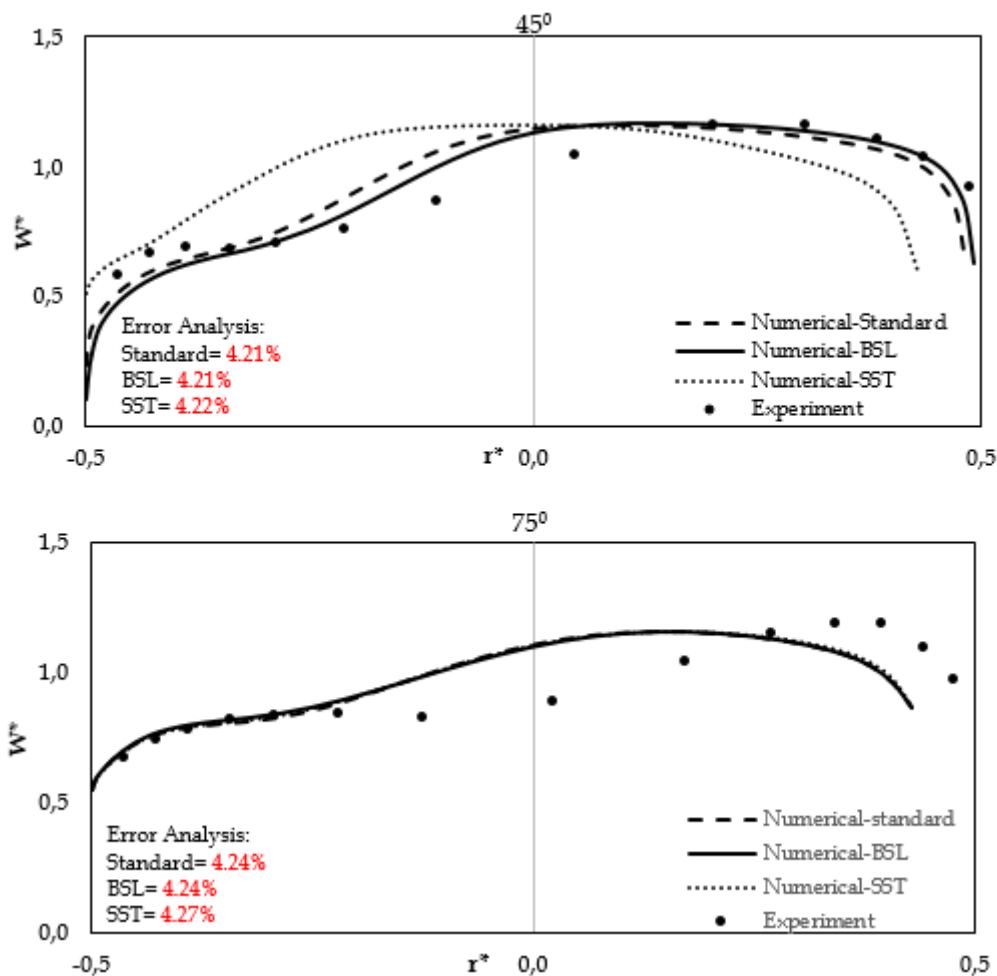


Figure 6: Normalized mean streamwise velocity plots obtained through the  $k - \omega$  turbulence models

The velocity profiles of the  $k - \omega$  models show similar accuracy compared to the  $k - \varepsilon$  models at 75° around the bend. At 45°, the  $k - \omega$  models (Standard and BSL) predict the experimental velocity profile better than the  $k - \varepsilon$  models.

### 3.3.3. Spalart-Allmaras model

The Spalart-Allmaras turbulence model solves one CFD equation and produces an average of flow viscosity. Figure 7 presents the streamwise velocities at 45° and 75° around the bend, obtained through the Spalart-Allmaras model, using the second-order discretization scheme.



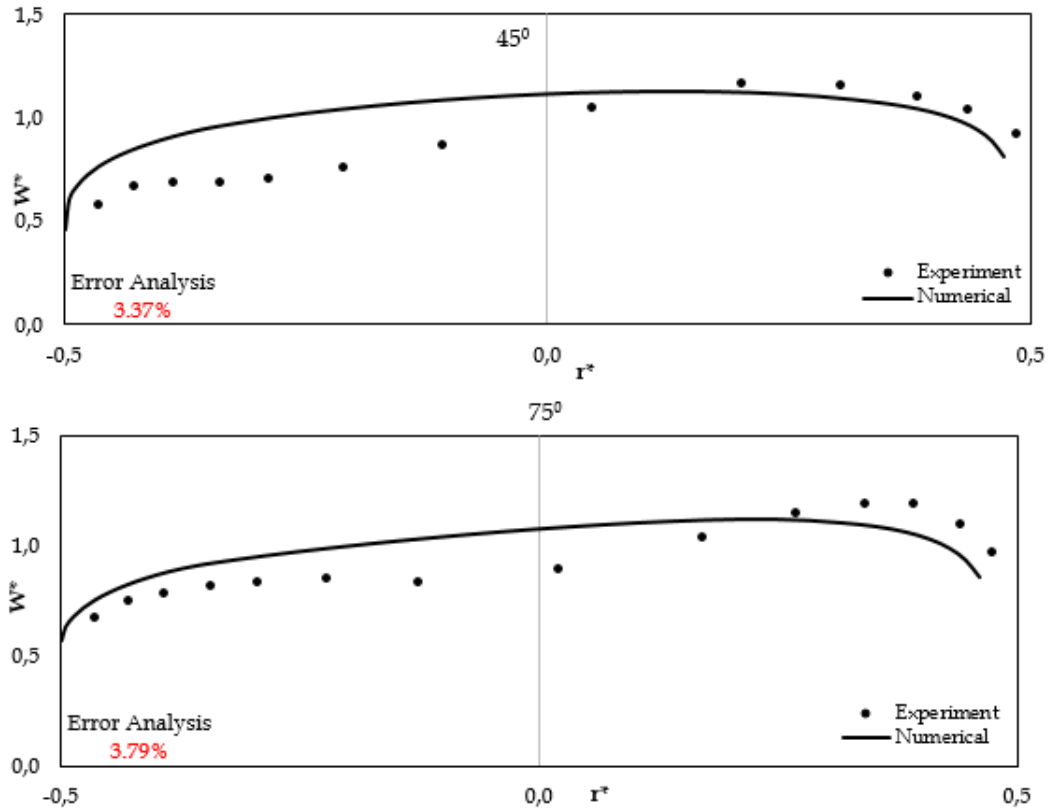


**Figure 7:** Normalized mean streamwise velocity plots obtained through the Spalart-Allmaras turbulence models

As observed from the plots, having a % errors of 3.37 and 3.79 at 45° and 75° respectively, the Spalart-Allmaras model outperforms all  $k - \varepsilon$  and  $k - \omega$  models in terms of the computed average errors. However in terms of the velocity curve, the Spalart-Allmaras model predicts the velocity profile similarly at 45° and 75° around the bend. In both cases, the predicted profiles deviate from the experimental profiles around  $r^* = -0.2$  to  $+0.1$ , which fall within the flow velocity transition zone. The Spalart-Allmaras can be effectively applied for low-Reynolds number model, however, with a properly resolved meshes of  $y^+$  approximately 1.

### 3.3.4. Transition SST model

The transition SST turbulence model is well suited for laminar flow situations transiting into a turbulent flow region, i.e. transitional flow. This fact though eliminates the eligibility of this model in this study, it is still necessary to understand the prediction capability of the model for the pipe bend under investigation.

The streamwise velocities at 45° and 75° around the bend, obtained through the transition SST model, using the second-order discretization scheme are presented in Figure 8. The transition SST model predicts the streamwise velocity of the flow with differences of 4.25% and 4.31% compared to the experimental measurements at 45° and 75° respectively. It was also observed (Figure 8) that the velocity profiles obtained through the transition SST model show similar accuracy compared to  $k - \omega$  models (Standard and BSL) at 45° and 75° around the bend. The model predicts the experimental velocity profiles more accurately than  $k - \varepsilon$  and Spalart-Allmaras models. The model solves 4 CFD equations/code and is applicable to wall bounded flow not for fully developed pipe flow, where no free-stream is present.

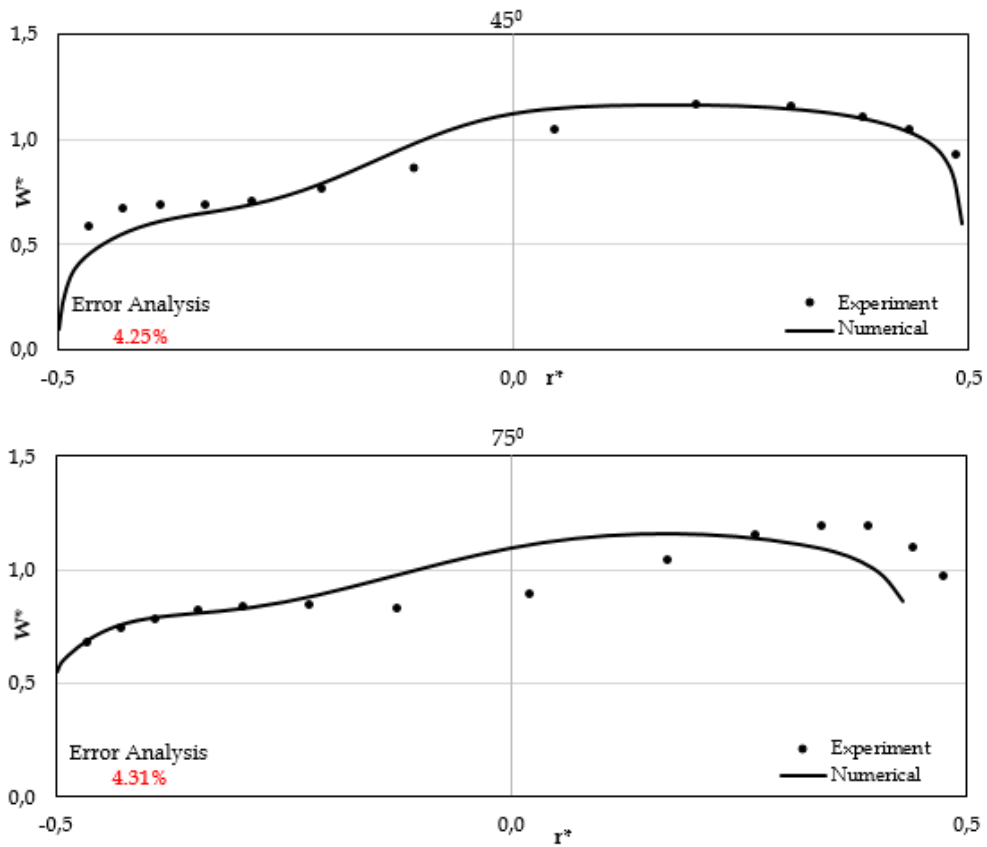


Figure 8: Normalized mean streamwise velocity plots obtained through the transition SST turbulence models

### 3.3.5. Reynolds stress model

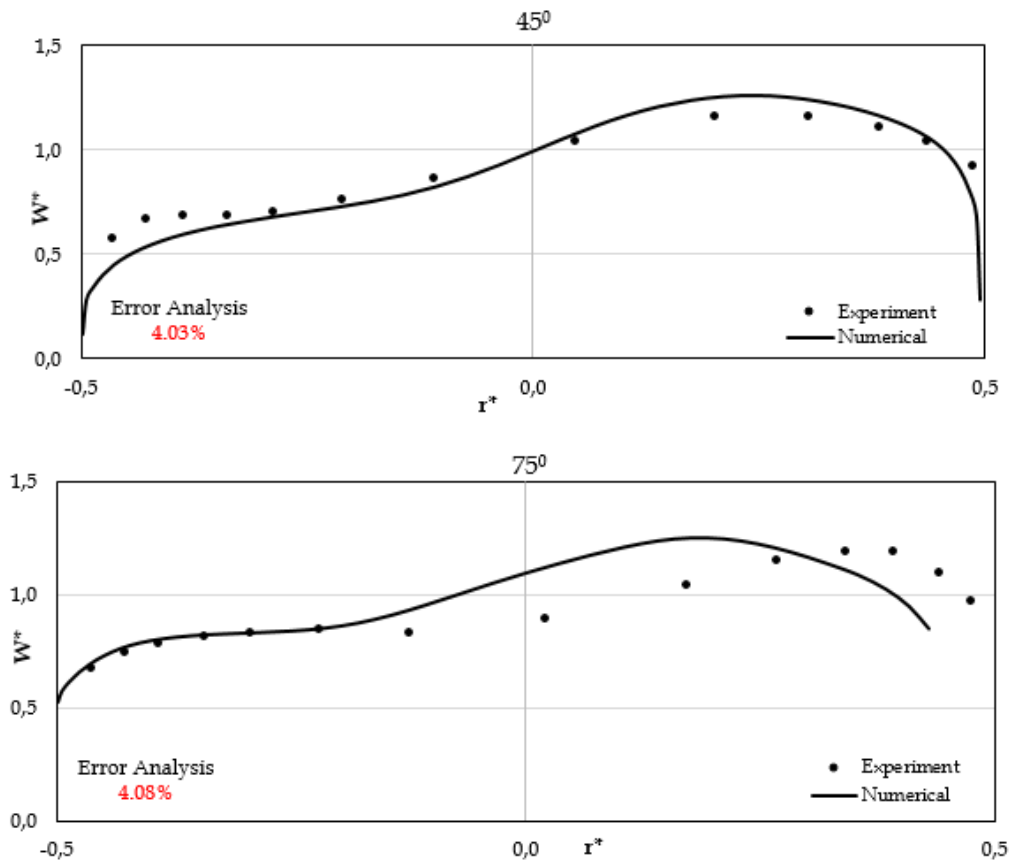


Figure 9: Normalized mean streamwise velocity plots obtained through the Reynolds stress turbulence models

The Reynold stress model is a 7 equations which is more computationally expensive than the 1 and 2 equation models, such as  $k - \varepsilon$  and  $k - \omega$  models. The model predicted the streamwise velocity magnitude around the bend to a satisfactory level as observed in Figure 9, with % average errors of 4.03 and 4.08 at 45° and 75° respectively.

The velocity profile obtained through the Reynold stress model at 45° around the bend is the best of all the investigated models, as it predicts the experimental velocity profile most accurately around  $r^* = -0.25$  to  $+0.2$ , which is the flow velocity transition zone.

### 3.3.6. Investigation of different spatial discretization schemes

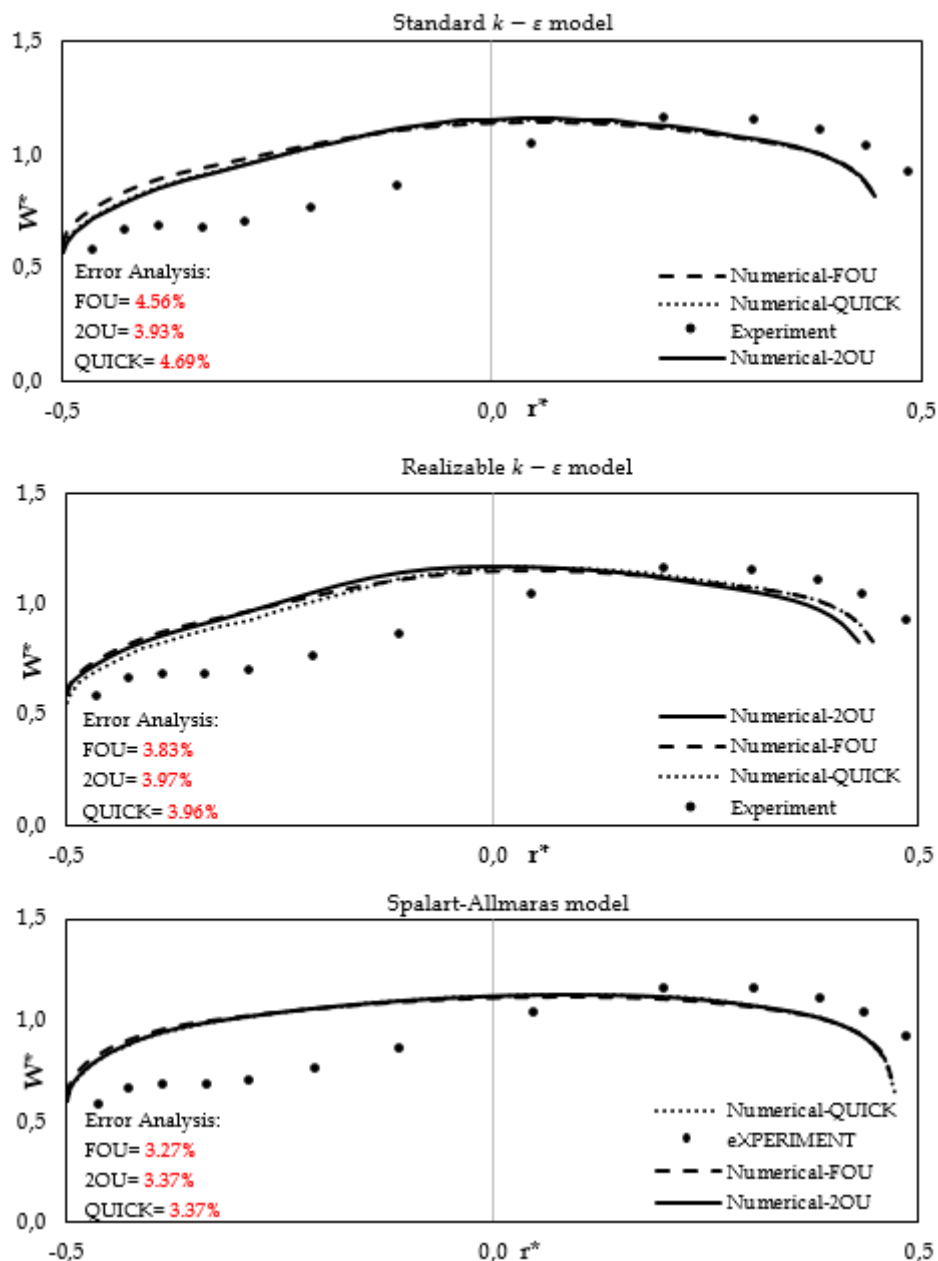


Figure 10: Normalized mean streamwise velocity plots for different turbulence models and different spatial discretization schemes

Having investigated the capabilities of the different turbulence models and established the best models for the present study case, using the second-order upwind spatial discretization scheme, it is necessary to further investigate the capabilities of the best models using the other discretization scheme. The  $k - \varepsilon$  and Spalart-Allmaras models, having exhibited the best

average errors, are investigated under the different spatial discretization schemes at 45° around the bend.

The streamwise velocities at 45° around the bend, obtained using the different discretization schemes for standard  $k - \epsilon$ , realizable  $k - \epsilon$  and Spalart-Allmaras turbulence models are presented in Figure 10. It is observed that the first-order upwind scheme produced the best accuracy, irrespective of the turbulence model used, except for the standard  $k - \epsilon$  model. Also, the Spalart-Allmaras model has the best accuracy in terms of the average error/difference (in comparison with the experimental measurements) for all the spatial discretization schemes, compared to all other turbulence models. The summary of the turbulence models error analyses is presented in Table 2: Summary of the turbulence models error analyses.

Turbulent Model	Discretization Schemes		
	FOU	2OU	QUICK
	% Error*		
Spalart-Allmaras	3.27	3.37	3.37
Standard $k - \epsilon$	4.56	3.93	4.69
RNG $k - \epsilon$	-	3.97	-
Realizable $k - \epsilon$	3.83	3.97	3.96
Standard $k - \omega$	-	4.21	-
BSL $k - \omega$	-	4.21	-
SST $k - \omega$	-	4.22	-
Transition SST	-	4.25	-
Reynold stress	-	4.03	-

\*Experimental measurement as reference; FOU – First-order upwind scheme; 2OU – Second-order upwind scheme

**Table 2:** Summary of the turbulence models error analyses

#### 4. Conclusions

In this study, different numerical turbulence models have been investigated for the computational fluid dynamics analysis of turbulent flow in 90° pipe bends. The turbulences models were studied using different spatial discretization schemes. The streamwise velocities of the turbulent flow, at cross-stream planes at 45° and 75° along the bend, were computed and the accuracies of the computations were measured against an existing experimental measurements. The main conclusions of the study are as follows:

- (i) The predicted streamwise velocity magnitude and flow physics satisfactorily agree with the experimental measurements, for all the models investigated, with a minimum and maximum average errors of 3.27% and 4.69% respectively.
- (ii) The Spalart-Allmaras turbulence model exhibited the best accuracy in terms of the average error (in comparison with the experimental measurements) among all the numerical turbulence models investigated, with the  $k - \epsilon$  model next in that order.
- (iii) In terms of the velocity profiles, the  $k - \omega$  (Standard and BSL), Transition SST and Reynolds Stress models exhibited the best correlation with the experimental velocity profiles, with the Reynolds Stress model exhibiting the best accuracy especially at 45° around the bend region.
- (iv) Considering the closeness of the average errors obtained through the different turbulence models, the velocity profiles predicted by the models exhibited a more significant variation compared to the average errors, especially within the velocity transition region.
- (v) In-depth understanding of the different turbulence models functionality and limitations has been established, in order to select appropriate model for specific simulation.

- (vi) As a future research, the study can be extended to transient simulation with LES-RANS model and with well-structured and refined meshes, a more accurate prediction of the flow physics can be achieved.

## References

- al-Rafai, W. N., Y. D. Tridimas, and N. H. Woolley. 1990. "A study of turbulent flows in pipe bends". *Proceedings of the Institution of Mechanical Engineers, Part C: Journal of Mechanical Engineering Science* 204, no. 6: 399-408. [https://doi.org/10.1243/PIME\\_PROC\\_1990\\_204\\_120\\_02](https://doi.org/10.1243/PIME_PROC_1990_204_120_02).
- Anwer, M., and R. M. C. So. 1990. "Frequency of sublayer bursting in a curved bend". *Journal of Fluid Mechanics* 210, no. 415: 415-35. <https://doi.org/10.1017/S0022112090001343>.
- Anwer, M., R. M. C. So, and Y. G. Lai. 1989. "Perturbation by and recovery from bend curvature of a fully developed turbulent pipe flow". *Physics of Fluids A* 1, no. 8: 1387-97. <https://doi.org/10.1063/1.857315>.
- Azzola, J., J. A. C. Humphrey, H. Iacovides, and B. E. Launder. 1986. "Developing turbulent flow in a u-bend of circular cross-section: Measurement and computation". *Journal of Fluids Engineering, Transactions of the ASME* 108, no. 2: 214-21. <https://doi.org/10.1115/1.3242565>.
- Boersma, B. J., and F. T. M. Nieuwstadt. 1996. "Large-eddy simulation of turbulent flow in a curved pipe". *Journal of Fluids Engineering, Transactions of the ASME* 118, no. 2: 248-54. <https://doi.org/10.1115/1.2817370>.
- Crawford, N. M., G. Cunningham, and S. W. T. Spence. 2007. "An experimental investigation into the pressure drop for turbulent flow in 90° elbow bends". *Proceedings of the Institution of Mechanical Engineers, Part E: Journal of Process Mechanical Engineering* 221, no. 2: 77-88. <https://doi.org/10.1243/0954408JPME84>.
- Di Piazza, I., and M. Ciofalo. 2010. "Numerical prediction of turbulent flow and heat transfer in helically coiled pipes". *International Journal of Thermal Sciences* 49, no. 4: 653-63. <https://doi.org/10.1016/j.ijthermalsci.2009.10.001>.
- Durbin, P. A., and B. A. Pettersson Reif. 2011. *Statistical Theory and Modeling for Turbulent Flows*. John Wiley & Sons, Ltd. <https://doi.org/10.1002/9780470972076>.
- Dutta, P., S. K. Saha, N. Nandi, and N. Pal. 2016. "Numerical study on flow separation in 90° pipe bend under high Reynolds number by k-ε modelling". *Engineering Science and Technology, an International Journal* 19, no. 2: 904-10. <https://doi.org/10.1016/j.jestch.2015.12.005>.
- Enayet, M. M., M. M. Gibson, A. M. K. P. Taylor, and M. Yianneskis. 1982. "Laser-Doppler measurements of laminar and turbulent flow in a pipe bend". *International Journal of Heat and Fluid Flow* 3, no. 4: 213-19. [https://doi.org/10.1016/0142-727X\(82\)90024-8](https://doi.org/10.1016/0142-727X(82)90024-8).
- Hellstrom, F., and L. Fuchs. 2007. "Numerical computations of steady and unsteady flow in bended pipes". In *Collection of Technical Papers - 37th AIAA Fluid Dynamics Conference*, 1850-59. <https://doi.org/10.2514/6.2007-4350>.
- Hilgenstock, A., and R. Ernst. 1996. "Analysis of installation effects by means of computational fluid dynamics - CFD vs experiments?". *Flow Measurement and Instrumentation* 7, no. 3-4: 161-71. [https://doi.org/10.1016/S0955-5986\(97\)88066-1](https://doi.org/10.1016/S0955-5986(97)88066-1).
- Homicz, G. F. 2004. *Computational Fluid Dynamic simulations of pipe elbow flow*. SAND2004-3467. United States: Sandia National Laboratories (SNL). <https://doi.org/10.2172/919140>.

- Kim, J., M. Yadav, and S. Kim. 2014. "Characteristics of secondary flow induced by 90-degree elbow in turbulent pipe flow". *Engineering Applications of Computational Fluid Mechanics* 8, no. 2: 229-39. <https://doi.org/10.1080/19942060.2014.11015509>.
- Lee, G. H., Y. D. Choi, and S. H. Han. 2007. "Measurement of developing turbulent flow in a U-bend of circular cross-section". *Journal of Mechanical Science and Technology* 21, no. 2: 348-59. <https://doi.org/10.1007/BF02916295>.
- Noorani, A. 2015. "Particle-laden turbulent wall-bounded flows in moderately complex geometries". PhD diss., TRITA-MEK, KTH Royal Institute of Technology. <http://urn.kb.se/resolve?urn=urn:nbn:se:kth:diva-177310>.
- Rahimzadeh, H., R. Maghsoodi, H. Sarkardeh, and S. Tavakkol. 2012. "Simulating flow over circular spillways by using different turbulence models". *Engineering Applications of Computational Fluid Mechanics* 6, no. 1: 100-09. <https://doi.org/10.1080/19942060.2012.11015406>.
- Röhrig, R., S. Jakirlić, and C. Tropea. 2015. "Comparative computational study of turbulent flow in a 90° pipe elbow". *International Journal of Heat and Fluid Flow* 55, no. C: 120-31. <https://doi.org/10.1016/j.ijheatfluidflow.2015.07.011>.
- Rowe, M. 1970. "Measurements and computations of flow in pipe bends". *Journal of Fluid Mechanics* 43, no. 4: 771-83. <https://doi.org/10.1017/S0022112070002732>.
- Schiestel, R. 2010. *Modeling and Simulation of Turbulent Flows*. John Wiley & Sons.
- Spedding, P. L., E. Benard, and G. M. McNally. 2004. "Fluid flow through 90 degree bends". *Developments in Chemical Engineering and Mineral Processing* 12, no. 1-2: 107-28. <https://doi.org/10.1002/apj.5500120109>.
- Sudo, K., M. Sumida, and H. Hibara. 1998. "Experimental investigation on turbulent flow in a circular-sectioned 90-degree bend". *Experiments in Fluids* 25, no. 1: 42-49. <https://doi.org/10.1007/s003480050206>.
- . 2000. "Experimental investigation on turbulent flow through a circular-sectioned 180-degree bend". *Experiments in Fluids* 28, no. 1: 51-57. <https://doi.org/10.1007/s003480050007>.
- Wallin, S., and A. V. Johansson. 2002. "Modelling streamline curvature effects in explicit algebraic Reynolds stress turbulence models". *International Journal of Heat and Fluid Flow* 23, no. 5: 721-30. [https://doi.org/10.1016/S0142-727X\(02\)00168-6](https://doi.org/10.1016/S0142-727X(02)00168-6).
- Wilcox, D. C. 1994. *Turbulence Modelling for CFD*. DCW Industries, Inc.